



HAL
open science

Cubane Cu₄I₄ (phosphine)₄ Complexes as New Coinitiator for Free Radical Photopolymerization: Towards Aromatic Amine-Free Systems

Fatima Hammoud, Mahmoud Rahal, Julien Egly, Fabrice Morlet-Savary,
Akram Hijazi, Stéphane Bellemin-Laponnaz, Matteo Mauro, Jacques Lalevée

► **To cite this version:**

Fatima Hammoud, Mahmoud Rahal, Julien Egly, Fabrice Morlet-Savary, Akram Hijazi, et al..
Cubane Cu₄I₄ (phosphine)₄ Complexes as New Coinitiator for Free Radical Photopolymeriza-
tion: Towards Aromatic Amine-Free Systems. *Polymer Chemistry*, 2021, 12 (19), pp.2848-2859.
10.1039/D1PY00277E . hal-03432108

HAL Id: hal-03432108

<https://hal.science/hal-03432108v1>

Submitted on 17 Nov 2021

HAL is a multi-disciplinary open access archive for the deposit and dissemination of scientific research documents, whether they are published or not. The documents may come from teaching and research institutions in France or abroad, or from public or private research centers.

L'archive ouverte pluridisciplinaire **HAL**, est destinée au dépôt et à la diffusion de documents scientifiques de niveau recherche, publiés ou non, émanant des établissements d'enseignement et de recherche français ou étrangers, des laboratoires publics ou privés.

Cubane Cu₄I₄(phosphine)₄ Complexes as New Co-initiator for Free Radical Photopolymerization: Towards Aromatic Amine-Free Systems

Fatima Hammoud^{1,2,3}, Mahmoud Rahal^{1,2,3}, Julien Egly⁴, Fabrice Morlet-Savary^{1,2}, Akram Hijazi³, Stéphane Bellemin-Lapponnaz⁴, Matteo Mauro^{4*} and Jacques Lalevée^{1,2*}

¹ Université de Haute-Alsace, CNRS, IS2M UMR7361, F-68100 Mulhouse, France.

² Université de Strasbourg, France.

³ EDST, Université Libanaise, Campus Hariri, Hadath, Beyrouth, Liban.

⁴ Université de Strasbourg, CNRS, Institut de Physique et Chimie des Matériaux de Strasbourg, UMR7504, 23 rue du Loess, 67000 Strasbourg (France).

Corresponding authors: mauro@unistra.fr; jacques.lalevee@uha.fr

Abstract:

The investigation of copper-iodide cubane derivatives as new co-initiators for the free radical polymerization (FRP) of acrylate monomers under mild irradiation conditions is described for the first time here. These tetranuclear Cu(I)-based complexes have general formula Cu₄I₄(phosphine)₄, where phosphine is triphenylphosphine (**Cu1**) or diphenylphosphine (**Cu2**). In the presence of commercial Type II photoinitiators such as isopropylthioxanthone (ITX) or camphorquinone (CQ), this class of co-initiators achieves high final conversions of the reactive functional groups. Comparison between the aromatic amine, such as ethyldimethylaminobenzoate (EDB) used as benchmark hydrogen donor, and these copper-based co-initiators are made, which demonstrates that the latter can be considered as a valid, environmental-friendly, alternative to toxic aromatic amines. Markedly, photoluminescent materials can be generated thanks to the presence of cubanes linked to the polymer network.

Keywords: copper complexes, co-initiator, free radical polymerization, photoinitiators, mild irradiation conditions, amine free system.

1. Introduction

Over the last decades, photopolymerization reactions have been used in many industrial applications, such as coatings, adhesives, (laser) imaging, composites, optics and dentistry, just to cite a few. These light-induced processes are milder and safer when compared to more widely-employed thermal processes, due to their reduced energy consumption and the use of low temperatures.^[1-5] Therefore, photopolymerization is considered a green technology because it may benefit of the use of safe light sources and there is low or no release of volatile organic compounds (VOCs) at room temperature condition.^[2-15]

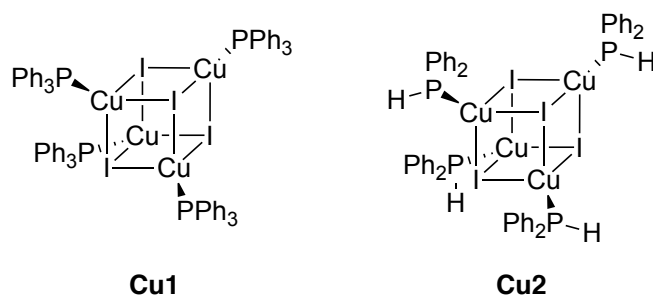
At industrial scale, both radical and cationic polymerization generally require high-intensity UV light sources, which can be dangerous for the human safety and are of environmental concern. On the other hand, light emitting diodes (LEDs) are ideal alternative light sources at both near-UV or visible range. These are safer, easily accessible and cheaper in terms of operating costs, power consumption and lamp lifetime.^[2,7-15] Nevertheless, the most widely employed photosensitive additives required UV light irradiation and alternatives are still limited. Therefore, the development of new and high-performance classes of photosensitive additives for efficient processes under visible light sources is highly desirable.^[10-17]

The photoinitiating systems are usually based on either Type I or Type II photoinitiators (PIs). A Type II photoinitiating system corresponds to a photochemically activated reaction between a PI and a co-initiator. It can then occur through either a hydrogen transfer reaction or an electron-proton transfer reaction.^[18] Most of the aromatic amines used as co-initiators, such as EDB, are now considered as toxic. Therefore, the search of safer photoinitiating systems is currently an important challenge in the field.^[18]

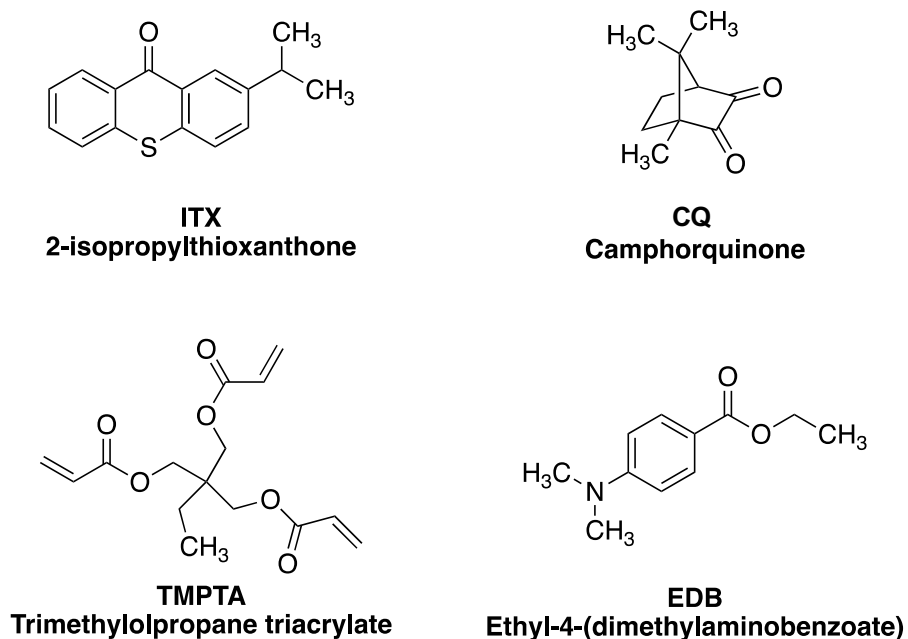
Photoactive metal complexes are currently subject of intensive research that is mainly driven by their appealing applications in the field of photocatalysis,^[19] solar energy conversion,^[20] and light emitting devices.^[21-25] In particular, tetranuclear copper-halide derivatives consisting of a tetranuclear cubane-like $\{\text{Cu}_4\text{X}_4\}$ motif, is a class of photoactive complexes with interesting optical properties.^[26-27]

In this work, metal complexes based on environment friendly and cheap copper(I) atoms of general formula $[\text{Cu}(\mu\text{-I})\text{L}]_4$ and where L = triphenylphosphine PPh_3 (**Cu1**) or diphenylphosphine HPPH_2 (**Cu2**) (Scheme 1) are tested as novel co-initiators in radical photopolymerization along with benchmark Type II photoinitiators (2-isopropylthioxanthone (ITX) or camphorquinone (CQ)

– Scheme 2). A comparison with reference photoinitiating systems based on aromatic amine (ethyldimethylaminobenzoate, namely EDB) is also provided. The chemical mechanisms are investigated through the combination of steady-state photolysis, laser flash photolysis and fluorescence experiments.



Scheme 1. Molecular structure of $[\text{Cu}(\mu\text{-I})\text{L}]_4$ copper complexes **Cu1** and **Cu2**.



Scheme 2. Molecular structure of other chemical compounds used in this study.

2. Experimental part

2.1. Synthesis of co-initiator

Synthesis of copper complexes Cu1 and Cu2

General procedure: copper(I) iodide (1 equiv.), phosphine (4 equiv.) and dry toluene were placed in a flame-dried Schlenk tube under argon (final concentration of copper *ca.* 0.5 M). The solution was heated at 100 °C for 24 hours. Then the mixture was cool down to room temperature and the solvent was removed under vacuum. The crude solid was dissolved in CH₂Cl₂ and the solution was poured into Et₂O. The complex precipitated instantaneously and was filtered and washed several times with Et₂O. The product was dried under vacuum. To ascertain the nature and the purity of compound **Cu2**, its Full chemical characterization of is provided as supplementary materials, including ¹H, ¹³C and ³¹P NMR and FT-IR spectra along with the X-ray power diffraction (XRPD), thermogravimetric (TGA) and differential scanning calorimetry (DSC) analysis (see Figure S1-S7).

Cu1: 65% yield starting from 1.0 g of CuI. The analyses were identical to the data previously reported for this compound. ^[24]

Cu2: 96% yield starting from 3.0 g of CuI. ¹H NMR (500 MHz, CDCl₃, 20 °C): δ 5.82 (d, *J* = 315.6 Hz, 4H), 7.18 (m, 16H), 7.26 (m, 8H), 7.49 (m, 16H) ppm; ¹³C NMR (125 MHz, CDCl₃, 20 °C): δ 128.57 (d, *J* = 9 Hz), 129.59, 130.32 (d, *J* = 29 Hz), 134.1 (d, *J* = 12.4 Hz) ppm; ³¹P NMR (202 MHz, CDCl₃, 20 °C) δ: -39 (br) ppm; Anal. Calcd for C₄₈H₄₄Cu₄I₄P₄: C, 38.27; H, 2.94; Found: C, 38.19; H, 2.79; FTIR: ν max (pure, diamond orbit) = 2975, 1476, 1437, 1089, 887, 819, 725, 686 cm⁻¹; TGA: 257°C 5% weight loss.

2.2. Other Chemical Compounds

All the other chemical compounds used in this work were selected with the highest purity available, their structures are shown in Scheme 2. 2-isopropylthioxanthone (ITX) was obtained from Lambson UK. Camphorquinone (CQ) was obtained from Tokyo Chemical Industry. Ethyl-4-(dimethylamino)benzoate (EDB) was purchased from Sigma Aldrich. Trimethylpropanetiacylate (TMPTA) was obtained from Allnex.

2.3. Irradiation Sources

The following light emitting diodes (LED) were used as irradiation source: i) $\lambda_{em} = 405$ nm (denoted LED@405 nm) with an incident light intensity at the sample surface: $I_0 = 110$ mW cm⁻²; ii) $\lambda_{em} = 455$ nm (denoted LED@455 nm); $I_0 = 100$ mW cm⁻².

2.4. Free Radical Photopolymerization

The two-component photoinitiating systems (PISs) are mainly based on commercial photoinitiator/cubane (1% / 1% w/w) compared with commercial photoinitiator/EDB (1%/1% w/w). The weight percent of the different chemical compounds in the photoinitiating system were calculated from the monomer content (w/w).

The FRP of TMPTA was done under laminate conditions (~25 μ m thickness) between two propylene films to reduce O₂ inhibition. The thick samples of (meth)acrylates (1.4 mm of thickness) were polymerized under air into a rounded plastic mold of 1 cm in diameter. For thin samples, the evolution of the double bond content was continuously followed by real time FTIR spectroscopy (JASCO FTIR 4100) at about 1630 cm⁻¹. The evolution of the (meth)acrylate characteristic peak for the thick samples was followed in the near-infrared range at ~6160 cm⁻¹. [25, 26, 27]

2.5. 3D Printing Experiments

For 3D printing experiments, a computer-controlled laser diode@405 nm (spot size of 50 μ m) was used for spatially controlled irradiation. The photosensitive resins with various thicknesses were polymerized under air and the generated 3D patterns were analyzed using a numerical optical microscope (DSX-HRSU from OLYMPUS Corporation). Further details can be found in previous references. [29-30]

2.6. Scanning Electron Microscopy Coupled with Energy-Dispersive X-ray Spectroscopy

A polymer was sliced using ultramicrotomy and analyzed using a JEOL, ARM200 transmission electron microscope (TEM) and SEM-EDX (FEI, Quanta 400).

2.7. Photo-rheology Experiments

A photorheometer was used to follow the storage modulus (G') in real time during the irradiation. For this type of rheometer, the product studied fills the space between two coaxial parts. It applies shear to the sample. The geometry used is a parallel plate (plane-plane).

2.8. Photophysical Characterization

Instruments. Electronic UV-visible absorption spectra during steady state photolysis experiments were performed using a JASCO V730 UV-visible spectrometer and baseline corrected. Steady-state emission spectra were recorded on a Horiba Jobin–Yvon IBH FL-322 Fluorolog 3 spectrometer equipped with a 450 W xenon arc lamp, doublegrating excitation, and emission monochromators (2.1 nm mm^{-1} of dispersion; $1200 \text{ grooves mm}^{-1}$) and a Hamamatsu R13456 red sensitive Peltier-cooled PMT detector. Emission and excitation spectra were corrected for source intensity (lamp and grating) and emission spectral response (detector and grating) by standard correction curves. Time-resolved measurements were performed using either the time-correlated single-photon counting (TCSPC) or the Multi Channel Scaling (MCS) electronics option of the TimeHarp 260 board installed on a PicoQuant FluoTime 300 fluorimeter (PicoQuant GmbH, Germany), equipped with a PDL 820 laser pulse driver. A pulsed laser diode LDH-P-C-375 ($\lambda_{\text{exc}} = 375 \text{ nm}$, pulse full width at half maximum FWHM $< 50 \text{ ps}$, repetition rate $200 \text{ kHz} - 40 \text{ MHz}$) was used to excite the sample and mounted directly on the sample chamber at 90° . The photons were collected by a PMA Hybrid-07 single photon counting detector. The data were acquired by using the commercially available software EasyTau II (PicoQuant GmbH, Germany), while data analysis was performed using the built-in software FluoFit (PicoQuant GmbH, Germany).

Methods. For time resolved measurements, data fitting was performed by employing the maximum likelihood estimation (MLE) methods and the quality of the fit was assessed by inspection of the reduced χ^2 function and of the weighted residuals. For multi-exponential decays, the intensity, namely $I(t)$, has been assumed to decay as the sum of individual single exponential decays (Eqn. 1):

$$I(t) = \sum_{i=1}^n \alpha_i \exp\left(-\frac{t}{\tau_i}\right) \quad (\text{Eqn. 1})$$

where τ_i are the decay times and α_i are the amplitudes of the components at $t = 0$. In the tables, the percentages to the pre-exponential factors, α_i , are listed upon normalization. Intensity average lifetimes were calculated by using the following equation (Eqn. 2):^[31]

$$\bar{\tau} = \frac{a_1\tau_1^2 + a_2\tau_2^2}{a_1\tau_1 + a_2\tau_2} \quad (\text{Eqn. 2})$$

2.9. Computational Methods

Molecular orbital calculations were carried out with the Gaussian 03 suite of programs.^[32] The structure was fully optimized in the density functional theory framework (at B3LYP/LANL2DZ level). The P-H bond dissociation energy (BDE) was calculated as the energetic difference between the radical and the starting molecule.

2.10. Redox potentials

The redox potentials (E_{ox} and E_{red}) were measured in dichloromethane by cyclic voltammetry using tetrabutylammonium hexafluorophosphate (0.1 M) as the supporting electrolyte (potential vs. Saturated Calomel Electrode – SCE). The free energy change ΔG_{et} for an electron transfer reaction was calculated from eqn (3),^[33] where E_{ox} , E_{red} , E_{T} , and C are the oxidation potential of the electron donor, the reduction potential of the electron acceptor, the triplet state energy of the excited state and the coulombic term for the initially formed ion pair, respectively. Here, C is neglected for polar solvents.

$$\Delta G_{\text{et}} = E_{\text{ox}} - E_{\text{red}} - E_{\text{T}} + C \quad (\text{Eqn. 3})$$

2.11. Laser Flash Photolysis Experiments

Nanosecond laser flash photolysis (LFP) experiments were carried out using a Q-switched nanosecond Nd:YAG laser ($\lambda_{\text{exc}} = 355$ nm, 9 ns pulses; energy reduced down to 10 mJ, Minilite Continuum) and an analyzing system consisting of a ceramic lamp, a monochromator, a fast photomultiplier and a transient digitizer (Luzchem LFP 212).^[34]

2.12. ESR Spin-Trapping (ESR-ST) Experiments

The ESR-ST experiments were carried out using an X-band spectrometer (Bruker EMX-plus). A LED@405 nm was used as irradiation source for the generation of radicals at room temperature (RT) under N₂ in *tert*-butylbenzene; the free radicals were trapped by phenyl-*N-tert*-butylnitrone (PBN) according to a procedure described elsewhere. [35,36] The ESR spectra simulations were carried out with the PEST WINSIM program.

3. Results and discussion

3.1. Photophysical properties of compounds Cu1 and Cu2

Firstly, the steady-state and time-resolved photophysical properties of complex **Cu2** were investigated in solution and in the solid-state as neat powder and compared with those of derivative **Cu1** reported elsewhere. [37] This is also in order to ascertain the suitability of the proposed copper-cubane complexes as active species in photopolymerization experiments. The UV-Visible absorption spectrum of the new proposed co-initiator (**Cu2**) in dilute dichloromethane (DCM) at room temperature is reported in Figure 1. **Cu2** displays a relatively high energy absorption onset that is estimated at $\lambda = ca.$ 385 nm. No intense absorption is present in the visible range and, in particular, in the region matching the emission spectrum of the visible LED lamp used in this work (*i.e.*, $\lambda_{exc} = 405$ nm and 455 nm, emission spectra are given in Figure S8), showing that this compound might only act as co-initiator and clearly requires the presence of a photoinitiator that will absorb near-UV or visible light.

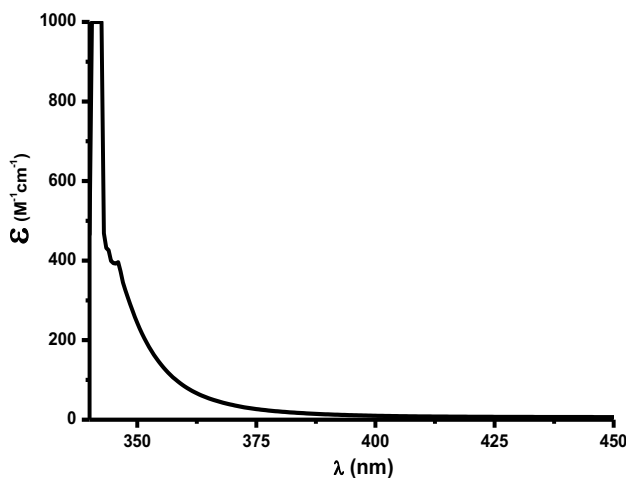


Figure 1. UV-Vis absorption of compound **Cu2** in dilute dichloromethane solution at room temperature.

Tetranuclear copper-iodide clusters with $\{\text{Cu}_4\text{X}_4\}$ cubane-type core and featuring four ligands located at each of the cubane vertex represent a valuable class of emitters, owing to their interesting photophysical properties, including dual emission arising from two electronically decoupled excited states, namely a high-energy (HE) $^3\text{XLCT}$, where $^3\text{XLCT}$ = triplet halide-to-ligand charge transfer, and a low-energy (LE) ^3CC , where ^3CC = triplet cluster-centered state.^[26b] Nevertheless, the vast majority of copper-halide clusters is emissive in aggregated state only, because of the high structural flexibility that largely favors non-radiative deactivation channels.^[38] Therefore, the photoluminescence properties of the compound **Cu2** were investigated in the solid-state as neat powder at both room temperature and 77 K, and the corresponding spectra are displayed in Figure 2.

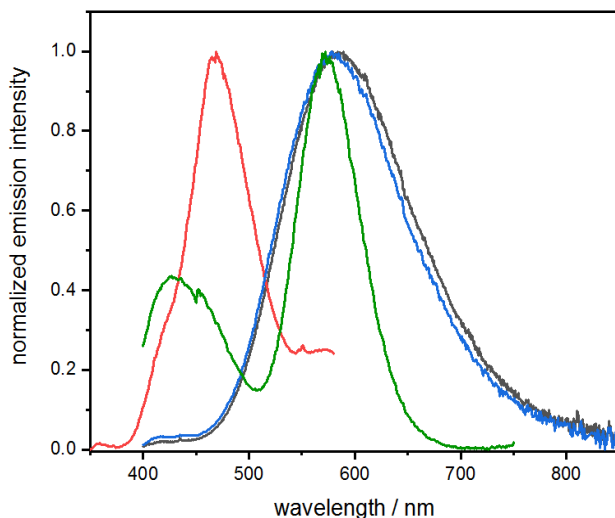


Figure 2. Photoluminescence spectra of compound **Cu2** as solid-state neat powder at room temperature upon $\lambda_{\text{exc}} = 300$ nm (black trace) and 340 nm (blue trace) as well as 77 K upon $\lambda_{\text{exc}} = 300$ nm (red trace) and 340 nm (green trace).

Upon photo-excitation, room-temperature solid samples of **Cu2** display a broad and featureless emission band with maximum centered at $\lambda_{\text{em}} = 583$ nm, independently of the excitation wavelength ($\lambda_{\text{exc}} = 300\text{--}340$ nm). This photoluminescence band is ascribed to an excited state with ^3CC nature also supported by the long-lived decay that can be fitted with a bi-exponential model, being $\tau_1 = 4.0$ μs (81%) and $\tau_2 = 1.6$ μs (19%). On the other hand, sample cooled down 77 K shows an excitation-dependent emission spectrum featuring dual emission, being $\lambda_{\text{em}} = 472$ and 574 nm

upon $\lambda_{\text{exc}} = 340$ nm. These two bands are ascribed to the two $^3\text{XLCT}$ and ^3CC excited states, respectively, with bi-exponential lifetime of $\tau_1 = 3.1 \mu\text{s}$ (48%) and $\tau_2 = 1.4 \mu\text{s}$ (43%), in agreement with previously reported investigations. [26]

3.2. Free Radical Photopolymerization of Acrylates (TMPTA)

3.2.1. FRP of Acrylates using ITX as Photoinitiator

Typical photopolymerization profiles for ITX-based photoinitiating systems, where the acrylate function conversion vs. time is plotted, are shown in Figures 3 (Figure S9). The data concerning the final acrylate function conversions (FCs) are also summarized in Table 1.

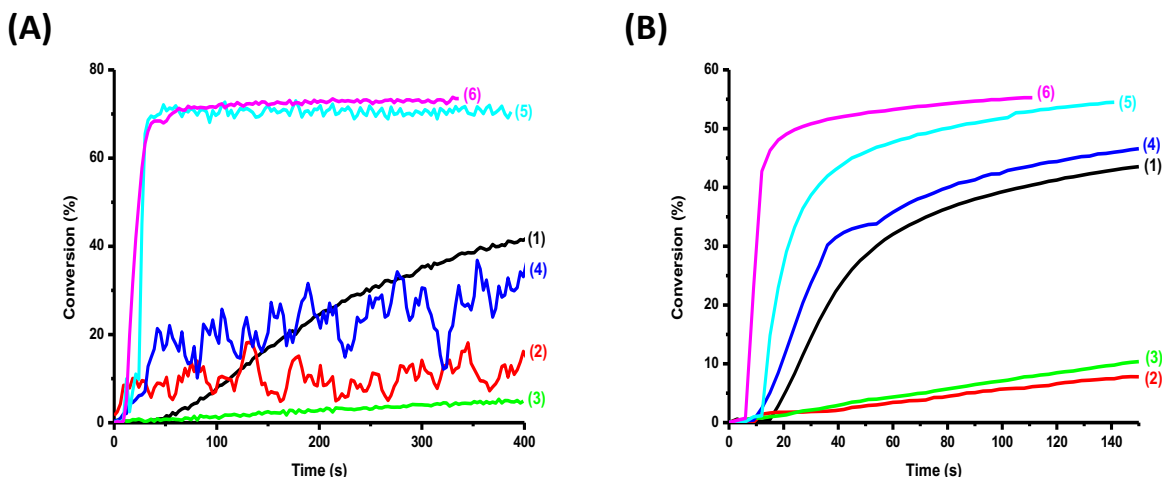


Figure 3. (A) Polymerization profiles of TMPTA (acrylate function conversion vs. irradiation time) under air (thickness= 1.4 mm) upon exposure to LED light $\lambda=405$ nm in the presence of one and two-component photoinitiating systems: (1) ITX: (1% w/w); (2) Cu1: (1% w/w); (3) Cu2: (1% w/w) (4) ITX\Cu1: (1%\1% w/w); and (5) ITX\Cu2: (1%\1% w/w); (6) ITX\EDB (1%\1% w/w); respectively. The irradiation starts for $t=10$ s. (B) Polymerization profiles of TMPTA (acrylate function conversion vs. irradiation time) in laminate (thickness= 25 μm) upon exposure to LED light $\lambda=405$ nm in the presence of one and two-component photoinitiating systems: (1) ITX: (1% w); (2) Cu1: (1% w); (3) Cu2: (1%) (4) ITX\Cu1: (1%\1% w/w); (5) ITX\Cu2: (1%\1% w/w); (6) ITX\EDB (1%\1% w/w); respectively. The irradiation starts for $t=10$ s.

Table 1. Final acrylate function conversion (FC) for TMPTA using different photoinitiating systems after 100 s of irradiation with LED light ($\lambda = 405$ nm). [a]

Thick sample (1.4 mm) under air						Thin sample (25 μm) in laminate					
ITX	Cu1	Cu2	ITX\Cu1	ITX\Cu2	ITX\EDB	ITX	Cu1	Cu2	ITX\Cu1	ITX\Cu2	ITX\EDB

42%	15%	5%	36%	71%	74%	44%	8%	10%	47%	55%	56%
-----	-----	----	-----	-----	-----	-----	----	-----	-----	-----	-----

^[a] All one and two-component photoinitiating systems were used in 1% w and 1%/1% w/w

For the FRP of TMPTA in thick samples (1.4 mm, under air), both systems **Cu1** alone and ITX/**Cu1** do not lead to efficient polymerization (Figure 3A; curves 2 and 4). Markedly, the ITX/**Cu2** (diphenylphosphine, HPPh₂) system is highly efficient (with both high polymerization rates (R_p) and high final conversion – Figure 3A, curve 5), this comparison between **Cu1** and **Cu2** clearly can show the importance of the presence of the labile hydrogen on the **Cu2** structure. Moreover, the ITX**Cu2** couple is quite efficient using the LED@405 nm (Figure S9 and Figure 3A; curve 5) compared to ITX or **Cu2** alone, for which almost no polymerization occurs (Figure 3A; curves 1 and 3, see also in Table 1). The efficiency of the ITX**Cu2** system clearly highlights the role played by **Cu2** as co-initiator.

The final acrylate function conversion (FC) of TMPTA monomer previously reached was about 37% with ITX alone and 5% with Cu₂ alone, whereas FCs as high as 71% are reached with the two-component photoinitiating system ITX**Cu2** (1%\1% w\w) under the same irradiation conditions.

Markedly, the same final conversion is obtained for this new co-initiator **Cu2** vs. the benchmark co-initiator EDB (Figure 3A; curve 5 vs. curve 6). The good performance of the ITX**Cu2** two-component systems is also well observed for thin samples (25 μm) as shown Figure 3B (curve 5) i.e. high polymerization rates (R_p) were also clearly achieved. Again, a better performance is noted in presence of the proposed co-initiator **Cu2**. As a matter of example, FC increases up to 55% with ITX**Cu2** (1%\1% w\w) compared with one component photoinitiating system that show an FC value of 42% with ITX alone and 10% with **Cu2** alone (Figure 3B, curves 1 and 3). In comparison with EDB, rather similar performance was achieved (Figure 3B, curve 6 for EDB vs. curve 5 with **Cu2**).

However, the molecular weight of the EDB (193.24 g/mol) is much lower than that of the **Cu2** compound (1506.58 g/mol), so if we want to compare their co-initiator ability for the same molar content, a much lower weight content of EDB must be used (0.13 %wt of EDB for 1 %wt of **Cu2**). The corresponding data are displayed in Figure 4.

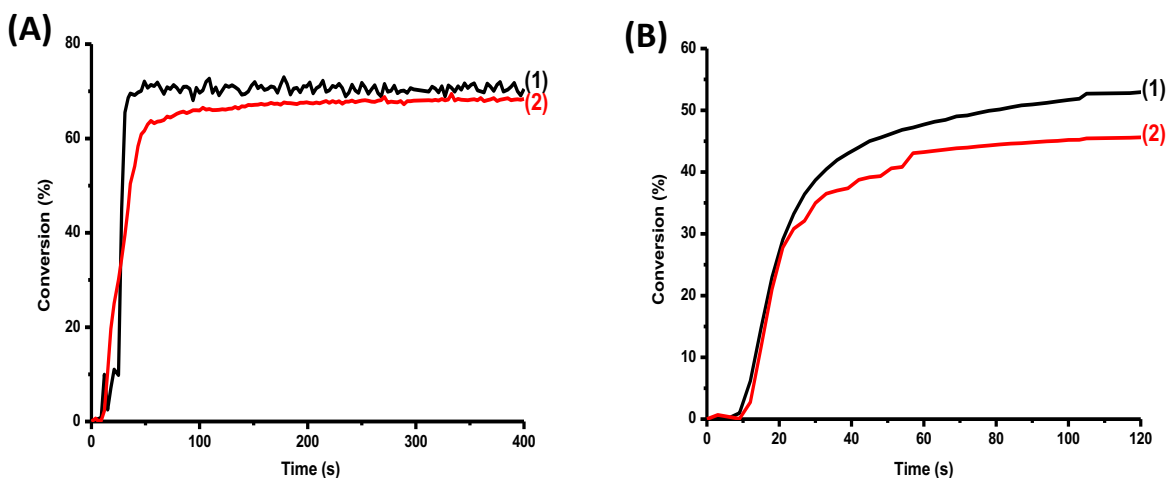


Figure 4. (A) Polymerization profiles of TMPTA (acrylate function conversion vs. irradiation time) under air (thickness = 1.4 mm) upon LED exposure ($\lambda = 405$ nm) in the presence of two-component photoinitiating systems: (1) ITX\Cu2 (1%1% w/w) and (2) ITX\EDB (1%0.13% w/w). The irradiation starts for $t = 10$ s. (B) Polymerization profiles of TMPTA (acrylate function conversion vs. irradiation time) in laminate (thickness = 25 μm) upon exposure to LED light $\lambda = 405$ nm in the presence of two-component photoinitiating systems: (1) ITX\Cu2 (1%1% w/w) and (2) ITX\EDB (1%0.13% w/w). The irradiation starts for $t = 10$ s.

Interestingly, a higher final conversion is obtained for the new co-initiator than that achieved with the benchmark amine EDB for thick and thin samples (Figure 4A and 4B, curve 1 vs. curve 2; see also in Table 2), showing that this co-initiator can be an interesting substitute for amines.

Table 2. Final acrylate function conversion (FC) for TMPTA using different photoinitiating systems after 100 s of irradiation with LED light $\lambda = 405$ nm.

Thick sample (1.4 mm) under air		Thin sample (25 μm) in laminate	
ITX\Cu2 (1%\1% w/w)	ITX\EDB (1%\0.13% w/w)	ITX\Cu2 (1%\1% w/w)	ITX\EDB (1%\0.13% w/w)
71%	65%	55%	45%

3.2.2. FRP of Acrylates using CQ as Photoinitiator

Typical photopolymerization profiles for CQ-based systems are displayed in Figure 5, and the associated final acrylate function conversion (FCs) are gathered in Table 3.

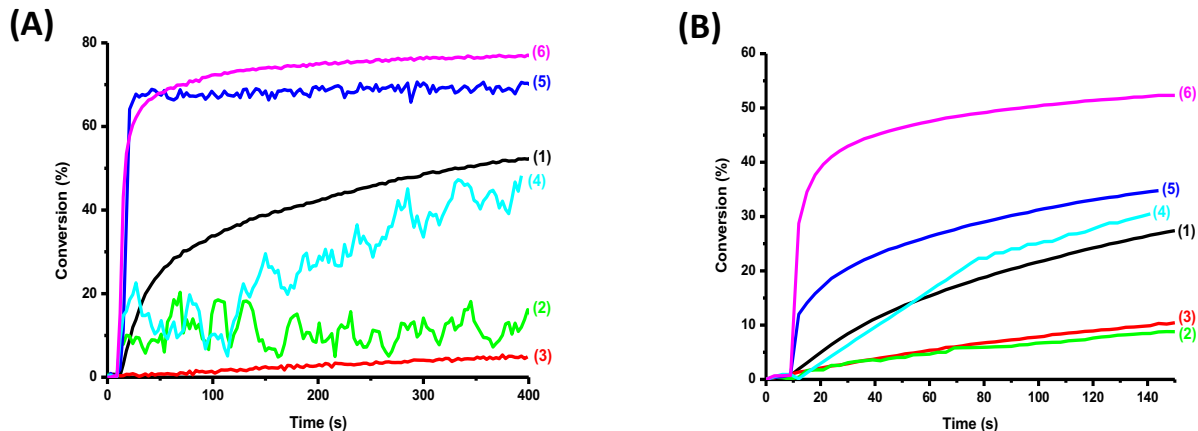


Figure 5. (A) Polymerization profiles of TMPTA (acrylate function conversion vs. irradiation time) under air (thickness= 1.4 mm) upon exposure to LED light $\lambda=455$ nm in the presence of one and two-component photoinitiating systems: (1) CQ (1% w/w); (2) Cu1 (1% w/w); (3) Cu2 (1% w/w); (4) CQ\Cu1 (1%\1% w/w); (5) CQ\Cu2 (1%\1% w/w) and (6) CQ\EDB (1%\1% w/w); respectively. The irradiation starts for $t=10$ s. (B) Polymerization profiles of TMPTA (acrylate function conversion vs. irradiation time) in laminate (thickness= 25 μm) upon exposure to LED light $\lambda=455$ nm in the presence of one and two-component photoinitiating systems: (1) CQ (1% w/w); (2) Cu1 (1% w/w); (3) Cu2 (1% w/w) (4) CQ\Cu1 (1%\1% w/w); (5) CQ\Cu2 (1%\1% w/w) and (6) CQ\EDB (1%\1% w/w); respectively. The irradiation starts for $t=10$ s.

Table 3. Final acrylate function conversions (FCs) for TMPTA using different photoinitiating systems after 100 s of irradiation with LED light $\lambda = 455$ nm.^[a]

Thick sample (1.4 mm) under air	Thin sample (25 μm) in laminate

CQ	Cu1	Cu2	CQ\Cu1	CQ\Cu2	CQ\EDB	CQ	Cu1	Cu2	CQ\Cu1	CQ\Cu2	CQ\EDB
52%	15%	5%	50%	71%	76%	28%	8%	10%	30%	35%	62%

^[a] All one and two-component photoinitiating systems were used in 1% w and 1%/1% w/w

The experimental results show the same reactivity of **Cu1** with CQ as with ITX, there is no polymerization noticed because of the absence of the labile hydrogen.

On the other hand, CQ\Cu2 system is quite efficient when using the LED@455 nm as a convenient mild irradiation source. Indeed, the FRP of TMPTA in thick films (1.4 mm, under air) in the presence of a two-component CQ\Cu2 system (1%/1% w/w) exhibits high efficiency in term of FC and polymerization rate. The efficiency is increased to reach FC = 71% with the two-component system CQ\Cu2 compared to only 52% for CQ alone and 5% for Cu2 alone (Figure 5A; curve 5 vs. curves 1 and 3; see also in Table 3).

Interestingly, the CQ\Cu2 (1%/1% w/w) system also initiate the FRP of TMPTA in thin samples (25 μ m, in laminate) (Figure 5B, curve 5). The maximum FC of TMPTA was about 28% with CQ alone and 10% with Cu2 alone compared to 35% to the two-component system CQ/Cu2 (1%/1% w/w) (Figure 5B, curves 1 and 3 vs. curve 5; Table 3). However, higher polymerization rates were observed for FRPs of thin samples in the presence of CQ\EDB system compared to CQ\Cu2 system (Figure 5B, curve 5 vs. curve 6).

3.3. 3D Printing Experiment using the ITX\Cu2 system

The good reactivity of **Cu2** as co-initiator allows the development of amine-free photoinitiating systems that can be used in 3D printing resins. 3D printing experiments upon light irradiation at 405 nm were successfully performed under air using ITX\Cu2 system in TMPTA (Figure 6). Indeed, the high photosensitivity of this system allows an efficient polymerization process in the irradiated area. Thick polymer samples were obtained with high spatial resolution and very short writing time, typically below one minute. 3D generated patterns were characterized by numerical optical microscopy (Figure 6). The spatial resolution is excellent and it is only limited by the size of the laser diode beam employed that has a spot size of 50 μ m.

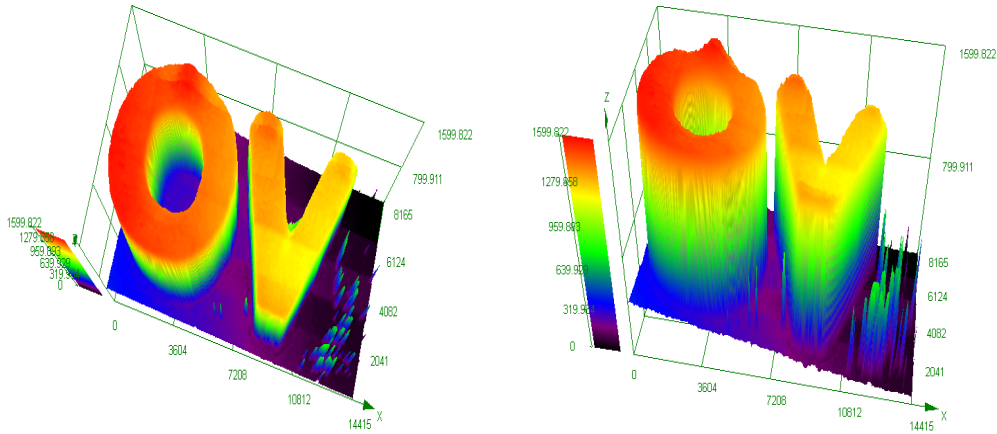


Figure 6. 3D patterns obtained upon exposure to a laser diode @405 nm: characterization by numerical optical microscopy; ITX\Cu₂ (1%\1% w\w) in TMPTA (thickness= 1599 μm).

3.4. Scanning Electron Microscopy/Energy-Dispersive X-ray Spectroscopy to characterize the polymers

Topological analyses were performed by SEM in order to compare the surfaces of polymers between the ITX\EDB and ITX\Cu₂ systems (Figure 7, image (A) with 1% EDB vs. image (B) with 1% Cu₂). It's interesting to notice the presence of the copper particles inside the polymer obtained from the ITX\Cu₂ system (Figure 7B'), showing the presence of the Cu₂ compound.

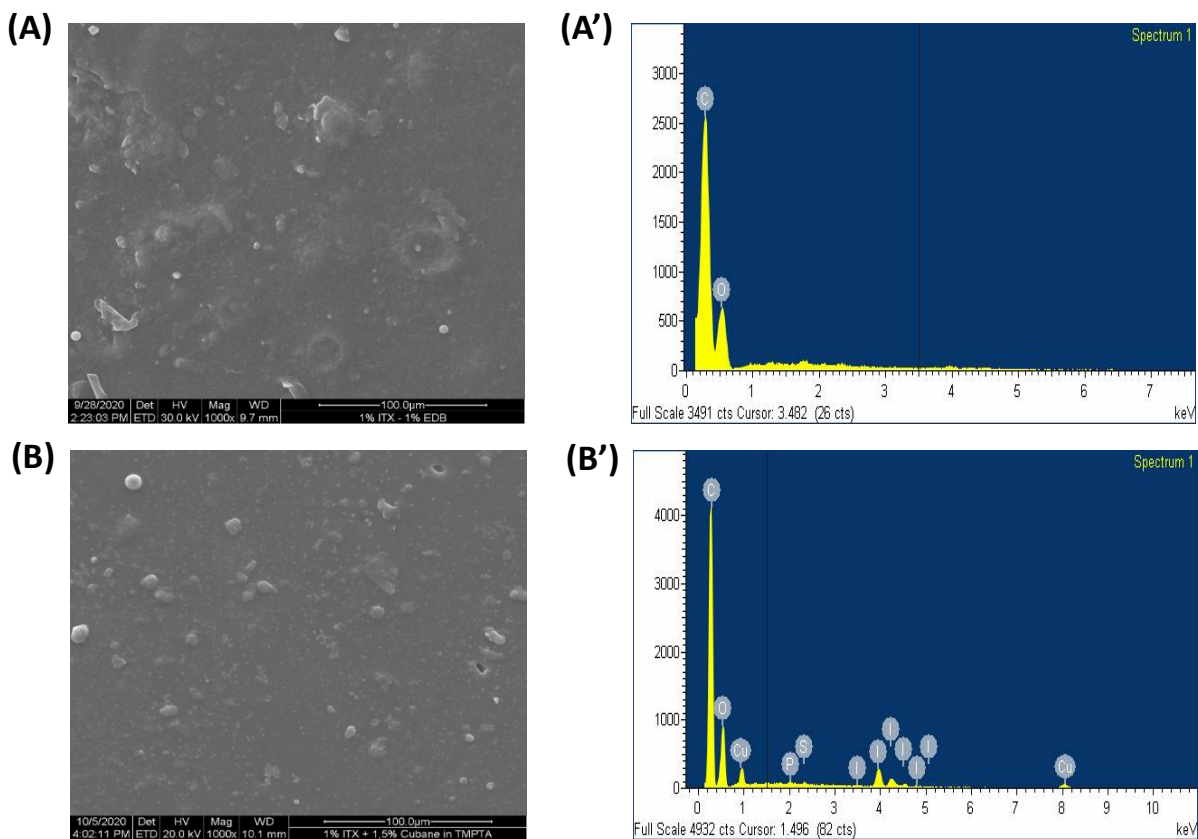


Figure 7. SEM micrographs of a polymer obtained from (A) ITX\EDB (1%\1% w\w) and (B) ITX\Cu₂ (1%\1% w\w) in TMPTA and the associated EDX spectra (A') and (B').

3.5. Photorheology Experiment

A dynamic rheometer is used to compare the rheological behavior of ITX/EDB and ITX/Cu₂ systems in TMPTA upon light irradiation. The photosensitive formulations were in situ irradiated in the photorheometer cavity with a LED@405 nm. The real-time characterization of the storage modulus G' obtained through oscillatory shear measurements during the photopolymerization process is depicted in Figure 8. All measurements were carried out in a plane-plane configuration (diameter = 5 mm) at room temperature.

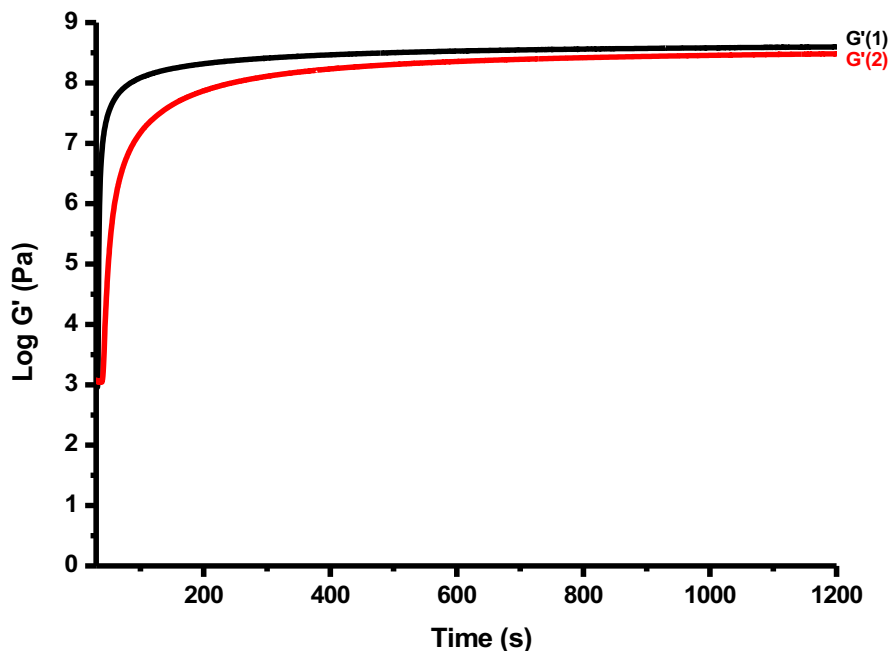


Figure 8. Dynamic rheological data: storage modulus (G') during the photopolymerization of: (1) ITX/EDB (1%/1% w/w) and (2) ITX/**Cu2** (1%/1% w/w); upon irradiation with a LED@405 nm; the irradiation starts for $t=10$ s at $T=25^{\circ}\text{C}$. Thickness of the investigated samples= 400 μm .

When the irradiation starts, the storage modulus (G') for the both systems ITX/EDB and ITX/**Cu2** rapidly increases. It's interesting to note that the final mechanical properties obtained for this new co-initiator are very similar than those of the benchmark co-initiator (Figure 8, curve 1 vs. 2; Table S1).

3.6. Cubane-based Photoluminescent Polymers

The use of cubane **Cu2** complex to initiate the polymerization allows the formation of composites with such entities covalently linked to the polymer network through reactivity at the P–H site of the coordinated diphenylphosphine. The peculiar and enhanced photophysical properties of copper-cubane clusters in the solid state ^[26] prompted the investigation of the emission properties of the printed polymers. The corresponding photoluminescence spectrum of the generated polymers after photopolymerization (e.g. using the ITX**Cu2** (1%\1% w\w) system in TMPTA) at room temperature is displayed in Figure 9. The spectrum showed an emission profile that clearly resemble that of cubane complex **Cu2** in solid state with only a small shift caused by the different environment compared to neat powder. This result shows the role of the **Cu2**

compound not only as a co-initiator, but also as a solid-state emitter, which can give multifunctional 3D-printed polymers with photoluminescent properties.

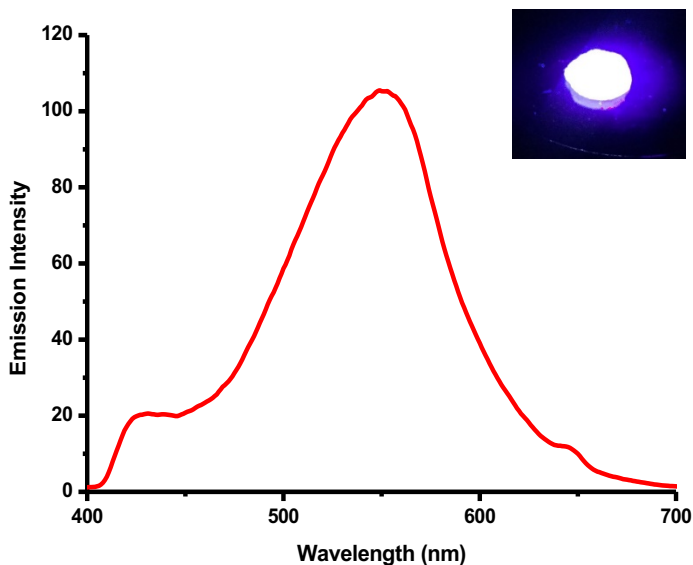


Figure 9. Photoluminescence spectrum upon $\lambda_{\text{exc}} = 320$ nm of a composite obtained by photopolymerization using the ITX\Cu2 (1%\1% w/w) system in TMPTA. Insert: photo of the TMPTA based polymer containing 1% w/w of Cu2 upon a Hg lamp irradiation.

3.7. Chemical Mechanisms

3.7.1. Steady State Photolysis

The photolysis of an ITX\Cu2 system is carried out in dichloromethane upon irradiation with a LED@375 nm. It's remarkable that there is efficient photolysis with fast formation of photoproducts after 240 s for the ITX\Cu2 system, compared to either Cu2 or ITX alone for which no photolysis occurs (Figure 10 C vs. A and B). This suggests a photochemical reaction between ITX and Cu2 in agreement with its co-initiator behavior observed above in photopolymerization experiments

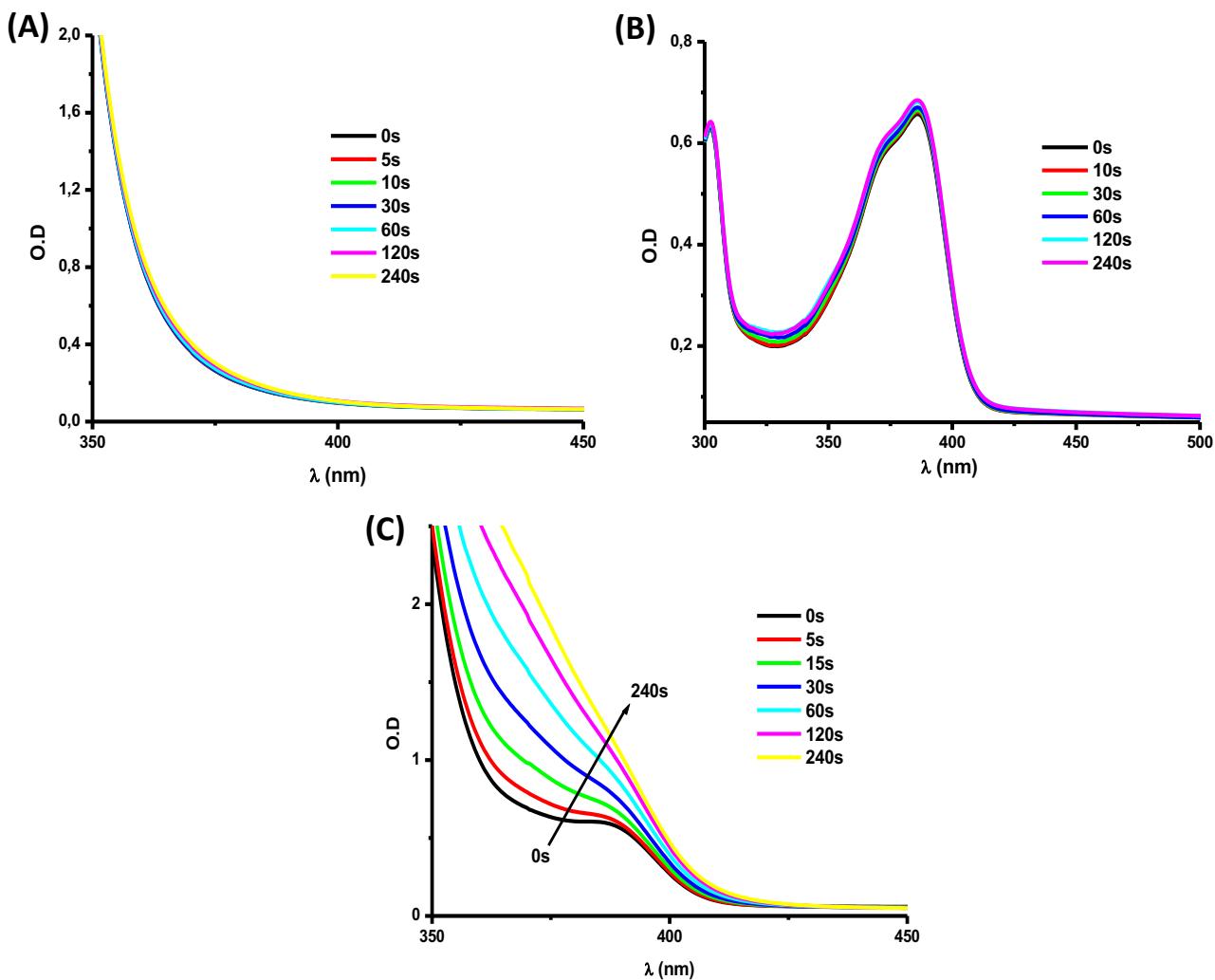
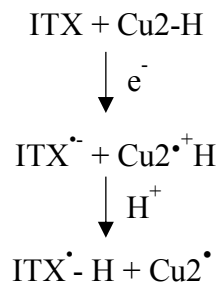


Figure 10. (A) Photolysis of Cu₂ alone; (B) Photolysis of ITX alone and (C) Photolysis of ITX/Cu₂; upon LED@375 nm in DCM.

3.7.2. Excited State reactivity

The free energy change (ΔG_{et}) for the electron transfer reaction between **Cu1** or **Cu2** as an electron donor and ITX or CQ as an electron acceptor was calculated from the classic eqn (1). The redox potential of **Cu1** has been measured by cyclic voltammetry (0.77 V). Using a reduction potential of -1.57 V and a triplet state energy of 2.74 eV for ITX while for CQ a reduction potential

of -1.4 V and a triplet state energy of 2.2 eV, the free energy change for the electron transfer reaction is $\Delta G_{et} = -0.4$ eV with ITX and -0.03 eV with CQ. In addition, the redox potential of **Cu2** has been also measured (0.38 V). the free energy change for the electron transfer reaction is $\Delta G_{et} = -0.79$ eV with ITX and -0.42 eV with CQ. This result suggests that the primary $^3\text{ITX}\backslash\text{Cu2}$ or $^3\text{CQ}\backslash\text{Cu2}$ interaction probably corresponds to an electron transfer reaction followed by proton transfer (Scheme 3).



Scheme 3. Electron-proton transfer reaction.

3.7.3. Laser Flash Photolysis (LFP) study

To study the hydrogen transfer process, laser flash photolysis experiments were carried out. On laser excitation of ITX in the presence of **Cu2** in dichloromethane, a quenching of ^3ITX is observed and its lifetime is strongly reduced (Figure 11A; Figure S10). The generation of ketyl radical ($\text{ITX}^{\cdot-}\text{-H}$ detected at 460 nm) is also observed (Figure 11B). The corresponding interaction rate constant was extracted from usual Stern-Volmer plots and equal to $10^{10} \text{ M}^{-1}\text{s}^{-1}$ for this $^3\text{ITX}\backslash\text{Cu2}$ interaction. This outlines the labile hydrogen character of the **Cu2** because ketyl radical ($\text{ITX}^{\cdot-}\text{-H}$, Scheme 3) is clearly observed and the phosphorus centered radicals associated with P-H hydrogen abstraction from **Cu2** are observed in ESR experiments - see below. This latter interaction rate constant is higher than those usually encountered in the $^3\text{ITX}\backslash\text{amine}$ systems, where an electron transfer process occurs (in the $10^8\text{-}10^9 \text{ M}^{-1}\text{s}^{-1}$ range).^[35, 39]

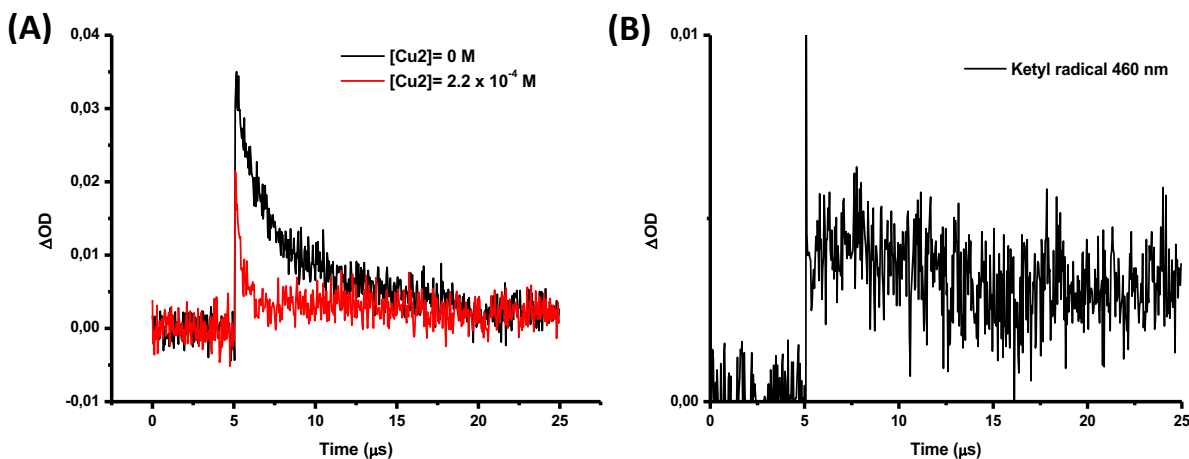


Figure 11. (A) Quenching of ³ITX observed at 600 nm with and without Cu₂ and (B) Generation of ketyl radical detected at 460 nm.

3.7.4. ESR Spin-Trapping (ESR-ST) Experiments

To better characterize this hydrogen abstraction process and more particularly the abstraction site and the kind of radicals generated, ESR spin trapping experiments were carried out. When a ITX\Cu₂ solution was irradiated in the presence of PBN, the ESR signal ($a_N = 14.4_4$ G; $a_H = 3.6_7$ G; $a_p = 16.4_3$ G) can be assigned to the trapping of phosphorus centered radicals (P[•]) by PBN (Figure 12). This unambiguously shows that phosphorus radicals are generated by hydrogen abstraction from Cu₂.

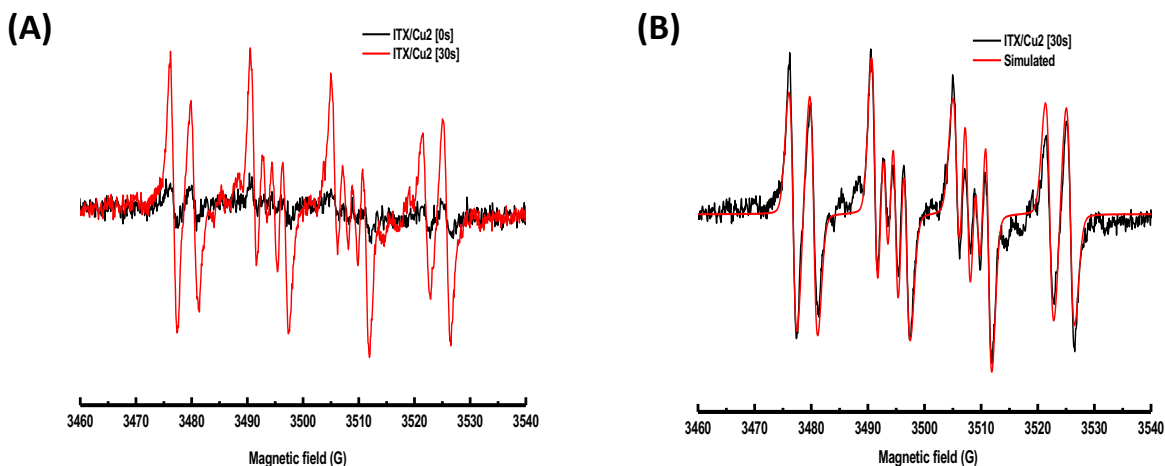
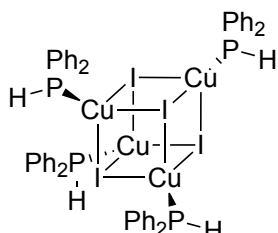
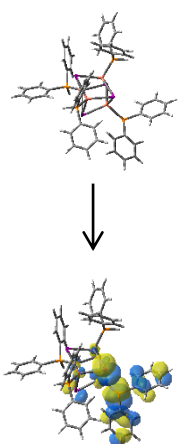


Figure 12. ESR spectra recorded for ITX\Cu2 solution in the presence of PBN in dichloromethane: (A) before and after irradiation (at t= 0s and t= 30s). (B) Simulated and experimental observed after irradiation (at t=30s).

3.7.5. Molecular Orbital Calculations

Molecular modelling was used to evaluate the P-H bond dissociation energy (BDE) in **Cu2**. Density functional theory calculations show that the BDE of the P-H bond is at 73.6 kcal mol⁻¹ (Table 4). This BDE is lower than the C-H bond of the EDB (96.7 kcal mol⁻¹).^[18] This rather low P-H BDE is in agreement with LFP and ESR data and favorable hydrogen abstraction process (Scheme 3).

Table 4. DFT calculations of the P-H bond dissociation energy; visualization of the SOMO for the P[•] radical.

Method uB3LYP/LANL2DZ	SOMO Isoval = 0.02	BDE (kcal mol ⁻¹)
 <p>Cu2</p> <p>Mol C₄₈ H₄₄ Cu₄ I₄ P₄</p>		73.57

4. Conclusion

In this article, a P-H functionalized copper-iodine cubane cluster (**Cu2**) was investigated as new co-initiator in photopolymerization reactions and compared to the benchmark derivative **Cu1** bearing PPh₃ ligands instead. The synthesis of **Cu2** as well as its initiation ability in combination with commercial Type II photoinitiators (isopropylthioxanthone ITX and camphorquinone CQ) are reported and thoroughly investigated by means of different spectroscopically techniques. The

results indicate that the P–H functionality in **Cu2** plays pivotal role in the light-induced process. The comparison with benchmark amines (such as EDB) has shown that the novel co-initiator **Cu2** complex is an interesting alternative for amine-free Type II photoinitiating systems. Markedly, a coherent picture of the chemical mechanisms is provided. This work paves the way for the further investigation of copper-iodide clusters as alternative classes of co-initiators in photopolymerization and novel advances will be proposed in forthcoming papers.

Acknowledgments. Institut Carnot Mica for the grant Pt4Poly. Dr. B. Heinrich is kindly acknowledged for help with the XRPD, TGA and DSC analyses.

5. References

- [1] J. P. Fouassier, *Photoinitiator, Photopolymerization and Photocuring: Fundamentals and Applications* Gardner Publications: New York, 1995.
- [2] J. P. Fouassier, J. Lalevée, *Photoinitiators for Polymer Synthesis, Scope, Reactivity, Efficiency*; Wiley-VCH Verlag GmbH & Co.KGaA: Weinheim, Germany, 2012.
- [3] K. A. Dietliker, *Compilation of Photoinitiators Commercially Available for UV Today*, Sita Technology Ltd., London, 2002.
- [4] S. Davidson, *Exploring the Science, Technology and Application of UV and EB Curing*, Sita Technology Ltd., London, 1999.
- [5] J. V. Crivello, K. Dietliker, G. Bradley, *Photoinitiators for Free Radical Cationic & Anionic Photopolymerisation*, John Wiley & Sons: Chichester, U. K., 1999.
- [6] W. A. Green, *Industrial Photoinitiators: A Technical Guide*, CRC Press, 2010.
- [7] M. U. Kahveci, A. G. Yilmaz, Y. Yagci, in *Photochemistry and Photophysics of Polymer Materials*, ed. N. S. Allen, John Wiley & Sons, Inc., 2010, 421–478.
- [8] B. Strehmel, T. Brömme, C. Schmitz, K. Reiner, S. Ernst, D. Keil, in *Dyes and Chromophores in Polymer Science*, (Eds.: J. Lalevée, J. P. Fouassier), John Wiley & Sons, Inc., 2015, 213–249.
- [9] Y. Yagci, S. Jockusch, N. J. Turro, *Macromolecules* 2010, 43, 6245–6260.
- [10] J. Lalevée, J. P. Fouassier, *Dye Photosensitized Polymerization Reactions: Novel Perspectives*, RSC Photochemistry Reports, Ed. A. Albini, E. Fasani, Photochemistry, London, UK, 2015, 215–232.
- [11] C. I. Vallo, S. V. Asmussen, In *Photocured Materials*; A. Tiwari, A. Polykarpov, Eds.; RSC Smart Materials Series 13, The Royal Society of Chemistry: Cambridge 2015, 321–346.
- [12] M. Abdallah, H. Le, A. Hijazi, M. Schmitt, B. Graff, F. Dumur, T.-T. Bui, F. Goubard, J. P. Fouassier and J. Lalevée, *Acridone derivatives as high performance visible light photoinitiators for cationic and radical photosensitive resins for 3D printing technology and for low migration photopolymer property*. *Polymer*, 2018, 159: 47-58.

- [13] J. Crivello, *Dyes and Chromophores in Polymer Science*, Ed. J. Lalevée, J. P. Fouassier, John Wiley & Sons, Inc., 2015, 45–79.
- [14] M. Sangermano, N. Razza, J. V. Crivello, *Cationic UV-curing: Technology and applications. Macromolecular Materials and Engineering*, 2014, 299.7: 775-793.
- [15] H. Mokbel, D. Anderson, R. Plenderleith, C. Dietlin, F. Morlet-Savary, F. Dumur and J. Lalevée, *Copper photoredox catalyst “G1”: A new high performance photoinitiator for near-UV and visible LEDs. Polymer Chemistry*, 2017, 8(36), 5580-5592.
- [16] J. Loccufier, *Polymerisable photoinitiators for LED curable compositions*, Patent No. US 8759412B2, 2014.
- [17] P. G. Odell, E. Toma, *Radiation curable inks*, Patent No. US 7838570B2, 2010.
- [18] E. Sprick, B. Graff, JM. Becht, T. Tigges, K. Neuhaus, C. Weber, J. Lalevée, *New bio-sourced hydrogen donors as high performance coinitiators and additives for CQ-based systems: Toward aromatic amine-free photoinitiating systems*, *European Polymer Journal*, 2020, 134, 109794.
- [19] J. Twilton, C. Le, P. Zhang, M. H. Shaw, R. W. Evans, D. W. C. MacMillan, *Nat. Rev. Chem.* 2017, 1, 52.
- [20] A. Hagfeldt, G. Boschloo, L. Sun, L. Kloo and H. Petterson, *Chem. Rev.*, 2010, 110, 6595.
- [21] E. Zysman-Colman, (Ed.), *Iridium (III) in optoelectronic and photonics applications*. John Wiley & Sons, 2017.
- [22] A. Barbieri, E. Bandini, F. Monti, V. K. Praveen and N. Armaroli, *The rise of near-infrared emitters: organic dyes, porphyrinoids, and transition metal complexes. Photoluminescent Materials and Electroluminescent Devices*, 2017, 269-307.
- [23] H. Yersin, (Ed.), *Highly efficient OLEDs with phosphorescent materials*. Weinheim: Wiley-VCH, 2008.
- [24] A. Barbieri, G. Accorsi, N. Armaroli, *Luminescent complexes beyond the platinum group: the d¹⁰ avenue*, *Chem. Commun*, 2008, 19: 2185-2193.

- [25] M. Wallesch, D. Volz, D. M. Zink, U. Schepers, M. Nieger, T. Baumann, and S. Bräse, Bright opportunities: Multinuclear CuI complexes with N–P ligands and their applications. *Chemistry–A European Journal*, 2014, 20.22: 6578-6590.
- [26] a) A. Kobayashi, M. Kato, Stimuli-responsive luminescent copper(I) complexes for intelligent emissive devices, *Chemistry Letters*, 2017, 46.2: 154-162; b) P. C. Ford, E. Cariati, J. Bourassa, *Chem. Rev.* 1999, 99 3625.
- [27] S. Perruchas, C. Tard, X. F. Le Goff, A. Fargues, A. Garcia, S. Kahlal, J.-Y. Saillard, T. Gacoin, and J.-P. Boilot, Thermochromic luminescence of copper iodide clusters: The case of phosphine ligands, *Inorg. Chem.*, 2011, 50.21: 10682-10692.
- [28] C. Dietlin, S. Schweizer, P. Xiao, J. Zhang, F. Morlet-Savary, B. Graff, J. P. Fouassier, J. Lalevée, Photopolymerization upon LEDs: new photoinitiating systems and strategies. *Polymer Chemistry*, 2015, 6.21: 3895-3912.
- [29] J. Lalevée, N. Blanchard, M. A. Tehfe, F. Morlet-Savary, J. P. Fouassier, Green bulb light source induced epoxy cationic polymerization under air using tris (2, 2'-bipyridine) ruthenium (II) and silyl radicals. *Macromolecules*, 2010, 43.24: 10191-10195.
- [30] J. Lalevée, N. Blanchard, M. A. Tehfe, M. Peter, F. Morlet-Savary, D. Gigmes, J. P. Fouassier, Efficient dual radical/cationic photoinitiator under visible light: a new concept. *Polymer Chemistry*, 2011, 2.9: 1986-1991.
- [31] J. Zhang, F. Dumur, P. Xiao, B. Graff, D. Bardelang, D. Gigmes, J. P. Fouassier and J. Lalevée, Structure design of naphthalimide derivatives: Toward versatile photoinitiators for near-UV/visible LEDs, 3D printing, and water-soluble photoinitiating systems. *Macromolecules*, 2015, 48.7: 2054-2063.
- [32] J. B. Foresman and A. Frisch, *Exploring chemistry with electronic structure methods: a guide to using Gaussian*, Gaussian Inc., Pittsburg. USA 2nd edn, 1196.
- [33] Lakowicz, J. R., ed. *Principles of fluorescence spectroscopy*. Springer science & business media, 2013.

- [34] P. Xiao, F. Dumur, J. Zhang, J.P. Fouassier, D. Gigmes, and J. Lalevée, Copper complexes in radical photoinitiating systems: applications to free radical and cationic polymerization upon visible LEDs. *Macromolecules*, 2014, 47, 3837-3844.
- [35] D. Rehm and A. Weller, Kinetics of Fluorescence Quenching by Electron and H-Atom Transfer, *Isr. J. Chem.*, 1970, 8, 259–271.
- [36] J. Lalevée, X. Allonas, and J. P. Fouassier, N– H and α (C– H) bond dissociation enthalpies of aliphatic amines, *Journal of the American Chemical Society*, 2002, 124(32), 9613-9621.
- [37] J. Lalevée, N. Blanchard, M. A. Tehfe, F. Morlet-Savary and J. P. Fouassier, Green Bulb Light Source Induced Epoxy Cationic Polymerization under Air Using Tris(2,2'-bipyridine) ruthenium(II) and Silyl Radicals, *Macromolecules*, 2010, 43, 10191–10195.
- [38] J. Lalevée, N. Blanchard, M. A. Tehfe, M. Peter, F. Morlet- Savary, D. Gigmes and J. P. Fouassier, Efficient Dual Radical/Cationic Photoinitiator under Visible Light: A New Concept, *Polym. Chem.*, 2011, 2, 1986–1991.
- [39] J. Lalevée, B. Graff, X. Allonas, and J. P. Fouassier, Aminoalkyl radicals: Direct observation and reactivity toward oxygen, 2,2,6,6-tetramethylpiperidine-N-oxyl, and methyl acrylate, *The Journal of Physical Chemistry A* 2007, 111 (30), 6991-6998.

TOC graphic:

